T2 mapping of cartilage in the equine distal interphalangeal joint with corresponding histology using 0.27 T and 3.0 T MRI

Baker Melissa (Orcid ID: 0000-0002-3684-4972)
Daniel Carola R (Orcid ID: 0000-0002-4801-5151)
Taylor Sarah (Orcid ID: 0000-0002-9714-8495)

T2 mapping of cartilage in the equine distal interphalangeal joint with corresponding histology using 0.27 T and 3.0 T MRI

Melissa E. Baker*[1], Lucy E. Kershaw[2], Ann Carstens[3], Carola R. Daniel[1], Helen Brown[1], Steve Roberts[4] and Sarah E. Taylor[1]

[1]Royal (Dick) School of Veterinary Studies and The Roslin Institute, The University of Edinburgh, Midlothian, UK; [2]Edinburgh Imaging and Centre for Cardiovascular Science, The University of Edinburgh, Edinburgh, Midlothian, UK; [3]School of Animal, Environmental and Veterinary Sciences, Faculty of Science, Charles Sturt University, Wagga Wagga, New South Wales, Australia and [4]Hallmarq Veterinary Imaging Ltd, Guildford, Surrey, UK.

*Corresponding author: Melissa Baker melissa.baker@ed.ac.uk

Keywords: horse, T2 mapping, cartilage, distal interphalangeal joint, MRI

Summary

Background: Low field MRI is widely available to equine veterinarians yet is insensitive at detecting cartilage damage in the distal interphalangeal joint (DIPJ). T2 mapping is a quantitative imaging technique that can detect cartilage damage before morphological change is apparent.

Objectives: Validation of a T2 mapping sequence on a low field MR system. Correlation of the mean T2 relaxation time in sections of cartilage with varying levels of pathology using low and high field MRI.

Study design: Cross sectional study.

Methods: Eight phantoms with known (nominal) T2 values underwent low field (0.27 T) MRI and 38 *ex vivo* DIPJs were imaged. A further 9 *ex vivo* DIPJs were imaged on both the low and high field MR system. Immediately after imaging, the DIPJs were disarticulated and samples collected for histology. Histological sections were graded using the OARSI scoring system. Fiji ImageJ software with the MRIAnalysisPak plugin was used to calculate T2 maps and draw the ROIs.

This article has been accepted for publication and undergone full peer review but has not been through the copyediting, typesetting, pagination and proofreading process which may lead to differences between this version and the Version of Record. Please cite this article as doi: 10.1111/evj.13900

Results: There was close agreement between the nominal and measured T2 values in the phantom study. Spearman's rank correlation demonstrated significant positive correlation between low and high field T2 measurements, rho 0.644 ($P < 0.001$). The intra-rater agreement for T2 measurements was excellent, ICC = 0.99 (95% CI = 0.99-1.00), the inter-rater agreement was excellent, ICC = 0.88 (95% CI = 0.82-0.92) and there was good intra-rater agreement for OARSI scores ($\kappa = 0.76$).
Main limitations: Only a small number of histological samples were analysed. Both articular cartilage surfaces were measured within the ROI. There were no OARSI grade 0 control samples.
Conclusions: A T2 mapping sequence on a low field 0.27 T MR system was validated. There was a positive correlation between low and high field T2 measurements. The findings suggest a higher mean T2 relaxation time in pathological cartilage tissue examined in this study compared to normal equine cartilage tissue.

1.0 Introduction

Osteoarthritis (OA) is a common musculoskeletal disease of the horse and is reported to be the most prevalent health problem in ageing horses; greater than 50% in horses >15 years and over 80% in horses >30 years [1]. It is a disease of diarthrodial joints characterised by variable levels of articular cartilage damage including matrix fibrillation, ulceration and cartilage loss along with subchondral bone sclerosis and osteophyte formation [2]. High motion joints of the equine distal limb are significantly affected by OA [2-4] with the distal interphalangeal joint (DIPJ) being commonly affected [5]. Joint degeneration causes pain, lameness, poor performance and often results in premature euthanasia [6,7]. Lameness is reported to be the primary cause for lost training days in racehorses [8-11] and causes major disruptions to training programmes leading to substantial economic losses to the equine sports industry [12], in addition to considerable welfare concerns.

Magnetic resonance imaging (MRI) has revolutionised diagnosis of musculoskeletal injuries in the equine distal limb over the past twenty years. Irregularities of the articular cartilage surface have been detected using both low (0.27 T) and high field (1.5 - 3.0 T) systems and the findings correlated with gross pathology and histological assessment in cadaver limbs [13-15]. However, both systems have been shown to have insufficient diagnostic ability to detect mild to moderate cartilage lesions before cartilage irregularities are evident. Currently, there are no diagnostic tools available for early detection of equine OA which has led to exploration of quantitative MRI techniques that detect tissue damage

before morphological change is apparent [16,17]. During cartilage deterioration the collagen and proteoglycan content decreases and is replaced by free water, increasing cartilage T2 relaxation time [18]. Several studies have used this technique in the human knee [19-21] but only a small number of studies have been performed in equine joints using high field systems. An experimental study measuring T2 relaxation time using a 1.5 T magnet on 10 horses after arthroscopic repair showed increased T2 relaxation time in reparative fibrocartilage compared to normal cartilage [22]. A longitudinal pony osteochondral model study investigating cartilage regeneration using a 3.0 T magnet demonstrated T2 relaxation time was significantly greater in the surgically created lesion compared to the adjacent cartilage and corresponded with increased collagen disorganisation [23]. Similar findings were also reported in another surgical osteochondral model study of the femoral condyle of four ponies [24]. Additionally, T2 relaxation times were significantly increased in the reparative tissue of osteochondral defects created in the lateral trochlear ridge of 12 adult horses [25] supporting the previous studies.

Low field 0.27 T standing magnets are the most widely available system in equine practice and have the significant advantage of negating the need for general anaesthesia for the patient. The study aimed to validate a T2 mapping sequence on a 0.27 T standing magnet and evaluate the mean T2 relaxation time in sections of cartilage with varying levels of pathology from histology determined by the OARSI (Osteoarthritis Research Society International) grading system [26] using low and high field MRI. The study then aimed to verify that our low field methodology generated similar T2 values to the high field system (3.0 T MR system). The hypothesis of the research was that higher mean T2 relaxation times would be found in cartilage with higher OARSI scores.

2.0 Materials and Methods

2.1 Case Selection

This was a cross sectional study. The horses were clinical cases seen at the R(D)SVS, Equine Hospital, University of Edinburgh which were euthanised due to several clinical diseases between 2019-2021. The first cohort of horses underwent low field MRI only and the second cohort underwent both low field and high field MRI. There was no standardised lameness examination performed prior to euthanasia. All cases included in the study had owners' consent for research purposes. A

convenience sample was used in this study as sample collection relied upon euthanasia of clinical cases in a set time period and owners' willingness to consent for use of those cases for research.

2.2 Imaging Acquisition

A 0.27 T open system (Hallmarq Veterinary Imaging Ltd©) was used to scan 8 phantoms (Figure 1) with known T2 values (Leeds Test Objects Ltd) for sequence validation, using a 2D multi echo gradient echo T2 mapping sequence (Table 1). The same 0.27 T system and T2 mapping sequence was used to image all *ex vivo* DIPJs in the study for low field MRI. The feet were positioned in the magnet to mimic a standing horse but not loaded. A 3.0 T clinical scanner (MAGNETOM Skyra 3T, Siemens Healthcare) was used for high field MRI, the position of the DIPJs mimicked the clinical scenario where the horse would be imaged in lateral recumbency under general anaesthesia. Table 1 shows the pulse sequence parameters for the T2 mapping sequence used, the most suitable echo times to measure cartilage T2 relaxation time were chosen.

The first cohort of 38 *ex vivo* DIPJs were imaged within 24 hours of euthanasia. Feet were removed by disarticulation at the metacarpophalangeal or metatarsophalangeal joint, synovial fluid was aspirated from the DIPJs and then the feet were placed in the standing magnet and imaged using the validated T2 mapping sequence. The limbs from the second cohort of 9 *ex vivo* DIPJs had been stored at -20°C prior to imaging. These feet were thawed at room temperature 24 hours prior to scanning in both the 0.27 T and 3.0 T MR systems.

2.3 Macroscopic and Microscopic Cartilage Assessment

Immediately after imaging, each DIPJ was opened by performing a circumferential cut above the coronary band and dissection through the collateral ligaments using a No.10 scalpel blade. The articular surfaces of the middle and distal phalangeal bones were inspected, photographed and sections of macroscopically normal and abnormal cartilage and subchondral bone were sampled at random using a cast saw in a sagittal plane. In addition, some samples were also deliberately taken from the lateral and medial articular surfaces of the middle and distal phalanx for comparison as the lateral condyle of the middle phalanx often demonstrated more gross pathological change than the medial condyle of the middle phalanx. Specimens were fixed in 10% neutral buffered formalin, immersed in Histo-Decal® for 7-10 days and then embedded in paraffin wax. Four-micron sections were cut and stained with haematoxylin and eosin and safranin O to assess the cartilage and

proteoglycan content. Sections were examined and graded twice by the same observer one month apart using the OARSI scoring system [26], which is the standard, validated histological scoring system used to assess human cartilage. Briefly, OARSI grade 0: surface intact, cartilage morphology and matrix intact. Grade 1: surface intact, oedema and/or superficial fibrillation of the superficial layer, cell death, proliferation and hypertrophy. Grade 2: surface and matrix discontinuity, safranin O stain depletion in the upper 1/3 of the cartilage tissue, cell death, proliferation and hypertrophy. Grade 3: vertical fissures, safranin O stain depletion into lower 2/3 of cartilage the cartilage tissue (middle and deep layers), cell death and hypertrophy.

2.4 T2 Mapping

Fiji ImageJ software [27,28] with the MRIAnalysisPak plugin [29] was used to calculate T2 maps by fitting a single exponential to the signal intensities on a voxel-by-voxel basis. Regions of interest (ROIs) were drawn over the articulating middle and distal phalanx cartilage on the TE=22 ms image slice (Figure 2) which matched the histological sample location. This was determined by measuring the length and width of the articular surfaces of the middle and distal phalanx in mm and matching the sample location to the correct corresponding image slice; there were 8 slices in total which were 3 mm thick.

Regions of interest were transferred to the T2 maps to calculate mean T2 relaxation time for the ROI drawn. This was repeated twice by one observer, an equine veterinary surgeon and once by a second observer, an equine veterinary surgeon and Diplomat of the European College of Veterinary Diagnostic Imaging (Dipl ECVDI). Observers were blinded to the macroscopic and microscopic scores of the ROIs and a reference document was used detailing the slice and position required for each ROI. The exact same method was used for the high field images, but the ROIs were drawn on the TE=14ms image slice.

2.5 Data analysis

Analyses were performed in GraphPad Prism version 9.0 for Windows (GraphPad Software, La Jolla California USA, www.graphpad.com) and R version 4.1.2 (R Foundation for Statistical Computing, Vienna, Austria, www.R-project.org). To evaluate the normality of the continuous T2 data and ordinal OARSI grade data, the Shapiro-Wilk test was used in GraphPad Prism version 9.0 followed by the Mann Whitney U test. Python version 3.10.5 (The Python Software Foundation, Delaware, USA, www.python.org) was used for the Wilcoxon signed-rank test. P values are indicated. The Mann

Whitney U test ($P < 0.05$) was used to measure the significance of differences in mean T2 measurements of medial compared to lateral ROIs and the Wilcoxon signed-rank test ($P < 0.05$) was used to determine significant differences for the corresponding OARSI grades. Correlation between low and high field T2 measurements was determined using Spearman rank correlation ($P < 0.05$) in R version 4.1.2. The inter and average intra-rater variability for T2 measurements was quantified using the intraclass correlation coefficient (ICC) in R version 4.1.2 using the 'psych' package in a two-way mixed effect model. The intra-rater variability for OARSI grades was analysed using Cohen's weighted kappa in R version 4.1.2 using the 'irr' package. ICC is widely used to assess intra-rater and inter-rater reliability with reliability defined as the extent to which measurements can be replicated [30]. Values of ICC greater than 0.90 are indicative of excellent reliability, between 0.75-0.90 good, between 0.50-0.75 of moderate reliability and less than 0.50 of poor reliability [30].

3.0 Results

Phantom Study

There was close agreement between the nominal and measured T2 relaxation times in the phantom study (Figure 3). Longer T2 values (>200 ms) were more difficult to measure precisely (shown by wider standard deviations) because the longest echo time for the sequence was 110 ms.

Cohort One

The first cohort of horses imaged on the low field MR system consisted of 19 horses: 3 stallions, 9 geldings and 7 mares, aged between 3-34 years (mean age of 12 years), weight range: 350-600 kg and included Warmbloods, Thoroughbreds, Irish Draughts, Standardbreds, Welsh ponies, Cobs, Connemara ponies and one Icelandic pony. The horses were subjected to euthanasia because of clinical disease which included colic, pituitary pars intermedia dysfunction, cervical vertebral malformation, lameness, congestive heart failure, incisional hernia and advanced dental disease. Two feet were imaged per horse.

The results of the mean T2 relaxation time for the 38 DIPJs scanned at low field for each OARSI grade are shown in Figure 4. Measurements include the first observers (Observer A) first (1) and second (2) measurements and the second observer's (Observer B) measurements. The intra-rater agreement for T2 measurements was excellent, ICC = 0.99 (95% confidence interval = 0.99-1.00) and

the inter-rater agreement was excellent, ICC = 0.88 (95% confidence interval = 0.82-0.92). In total, 80 histological slides (two slides per joint) were graded using the OARSI system twice by Observer A and the intra-rater agreement was good κ = 0.76 (95% confidence interval = 0.60-0.90). The sample set consisted of grade 0: 0 slides, grade 1: 36 slides, grade 2: 26 slides and grade 3: 18 slides.

The same histological samples from above which were specifically taken from the lateral (31 slides) and medial (31 slides) sections were compared and the results demonstrated a significant difference between the mean T2 relaxation time in the ROI measured in the lateral compared to the medial section of the joint. The mean T2 relaxation time was significantly increased ($P < 0.001$) in the lateral compared to the medial section. Figure 5 shows graphs of the lateral and medial T2 measurements recorded by each observer. There was no significant difference in mean OARSI grade in the lateral vs medial side of the joint (1.8 ±0.7 vs 1.6 ±0.7, Wilcoxon signed-rank test $P > 0.1$). Figure 6 demonstrates a left fore DIPJ case example which illustrates the gross pathology of the articulating middle and distal phalanx, histology from the lateral and medial middle phalanx and the corresponding T2 colour map of the image slice where the samples were taken. The T2 map colour overlay on the corresponding TE=22 ms image visually highlights the lateral and medial T2 relaxation time differences.

Cohort Two

The second cohort of horses consisted of 5 Thoroughbred racehorses which were used to image the DIPJ on both the low and high field MR system. There were 2 stallions and 3 geldings aged between 4-13 years (mean age 7 years). The horses had sustained injuries whilst racing: cervical vertebral fracture, lumbar vertebral fracture, fracture of the middle phalanx and complete open fracture of the right fore third metacarpal bone and were therefore subjected to euthanasia at the racecourse on humane grounds. Two feet from 4 horses and one foot from 1 horse were imaged.

The results of mean T2 relaxation time for the 9 DIPJs scanned at low and high field for each OARSI grade are shown in Figure 7 and Figure 8 shows a case example of a right fore DIPJ scanned on both the low and high field MR system. T2 measurements were repeated twice by the same observer which demonstrated an excellent intra-rater agreement, ICC = 0.96 (95% confidence interval = 0.91-0.98). In total 36 histological slides were graded (four slides per joint) using the OARSI system and

slides were graded twice by the same observer giving a good intra-rater agreement (κ = 0.75). The sample set consisted of grade 0: 0 slides, grade 1: 26 slides, grade 2: 6 slides and grade 3: 4 slides.

Spearman's rank correlation demonstrated significant positive correlation between low and high field T2 measurements, rho 0.644 ($P < 0.001$). Figure 9 shows a Bland-Altman plot of the T2 data from the low and high field T2 measurements (mean vs. difference between high and low field MRI). There was an overall bias of 15 ms between low and high field measurements with a standard deviation of 20 ms and a relatively wide 95% confidence interval of 80 ms, likely reflecting the difficulty of measuring longer T2 values with high precision.

4.0 Discussion

The research successfully implemented a T2 mapping sequence for the standing 0.27 T magnet MR system (Hallmarq Veterinary Imaging©), as demonstrated from the results of the phantom study which confirmed very close agreement for nominal and measured T2 values. To measure T2 relaxation time with precision, the echo times should be spaced in time to characterise the exponential decay of the signal, covering a drop from high signal down to low signal. In tissues with a long T2 value, the signal will not have decayed substantially by the longest echo time, so although a measurement of T2 relaxation time can be derived, it will not be very precise. There was a significant positive correlation between low and high field T2 measurements recorded in equine cartilage tissue, indicating that T2 measurements on 0.27 T low field MRI are comparable to 3.0 T high field for cadaveric equine DIPJs. The Bland-Altman plot did show a degree of bias which was to be expected, as T2 relaxation time is slightly different between the two field strengths however the agreement was positive. The authors did not identify magic angle artifact in the study at either high field or low field. Also, no freeze-thaw artifacts were identified in cohort two and freeze-thawing of equine cadaver limbs has been reported to have minimal effects on T1, T2 and STIR relaxation times [31,32].

The findings suggest a higher mean T2 relaxation time (83-104 ms) in pathological cartilage tissue examined in this study compared to normal equine cartilage tissue which is reported to range from 40-61 ms [22]. However, the T2 relaxation time did not increase with increasing OARSI grades as expected, for measurements in either the low or high field MR system. This may have been because we did not have large enough sample numbers for grade 2 and 3 to demonstrate a significant difference or may reflect the fact that the cohorts investigated did not have histological samples with a

OARSI grade 0, despite sampling from macroscopically normal articular cartilage. The sample population has, however, confirmed the difficulty with ascertaining a normal control group in clinical research and that macroscopically normal articular cartilage is often not histologically normal, which has been described for other equine joints [33]. There were no samples with an OARSI grade higher than 3 however, the mean T2 relaxation time would have been extremely difficult to measure in OARSI grades 4 and 5 due to little or no cartilage presence.

The results of the current study demonstrated that T2 relaxation time was significantly increased in lateral ROIs compared to medial ROIs of the DIPJ however there was not a significant difference between the OARSI grades between the lateral and medial sections. This finding might be due to inclusion of a higher volume of synovial fluid in the ROI in the lateral side of the joint. The data does not suggest that it is due to a higher OARSI score in the lateral sections, however since correlation does not imply causation, additional work would need to be performed before concluding that increased T2 relaxation time correlates with increased OARSI grades in the equine DIPJ cartilage anyway. For example, mixed effect modelling taking into account the horse's weight, age, breed, sex, stage of OA, lameness history and concurrent health problems would all need to be considered alongside the important limitation of synovial fluid being measured within the ROI before an accurate correlation could be determined. Moreover, we are currently constrained with image resolution in both systems and ideally need to be able to measure voxels containing only cartilage tissue ensuring that synovial fluid and subchondral bone is not incorporated. Also, interestingly exercise has been shown to decrease the T2 relaxation time in human knee cartilage [34,35] which would need to be considered when imaging live horses.

There was a common middle phalanx macroscopic lesion distribution found in this data set. Van Zadelhoff et al.'s research on naturally occurring cartilage damage in the equine DIPJ reported most cartilage defects were located at the lateral distal phalanx location followed by the lateral middle phalanx [5]. Advanced cartilage abrasion, fibrillation and discolouration appeared more frequently on the lateral condyle of the middle phalanx compared to the medial condyle. In addition, the lesions tended to be positioned centrally and palmarly rather than in the dorsal portion of the joint. Interestingly this is in contrast to the pattern distribution of OA in the metacarpophalangeal joint which was investigated in 73 right metacarpophalangeal joints from horses aged 5 months - 23 years [3]. The articular surface of the proximal phalanx was semi quantitatively scored on a 0 to 5 scale and

quantitatively assessed using the cartilage degeneration index (CDI) [36]. The CDI uses Indian ink particle uptake across the total cartilage surface and quantifies the ink-stained articular cartilage surfaces by digital imaging [37,38]. Degenerated cartilage is depleted of proteoglycans and undergoes surface fibrillation which absorbs the Indian ink particles compared to intact cartilage which is barely stained. CDI values were defined for specific areas of interest: medial dorsal surface, lateral dorsal surface, medial central fovea and lateral central fovea. The results showed CDI grading was higher in medial and dorsal compared to lateral and central areas confirming a specific pattern distribution which is likely influenced by biomechanical loading. The biomechanics of the DIPJ have been studied by several authors [39-42] and during straight line locomotion added motion outside the sagittal plane, such as lateral or medial motion and axial rotation, occurs to various extents due to changes in the mediolateral orientation of the hoof [39]. Alterations in lateral, medial and axial motion is mainly caused by asymmetric weight bearing, through uneven ground or poor mediolateral balance of the hoof [43,44] and this is likely to contribute to specific patterns of cartilage damage. Assessment of lesion distribution in the DIPJ was not an objective of this research, however this incidental finding certainly warrants further investigation using quantitative methods such as the CDI. Further insight into the pattern of cartilage degeneration will enable a better understanding of the dynamic nature and progression of OA in the DIPJ which can form a foundation for advancements in diagnostic and therapeutic approaches to OA. Important limitations to recognise are, firstly, only a small number of histological samples were analysed from each joint, therefore the sample examined may not represent all the cartilage tissue measured in the ROI. Secondly, constraints in image resolution meant ROIs were drawn over two cartilage surfaces (the middle and distal phalanx) inevitably incorporating synovial fluid which impacts T2 relaxation time and is the main limitation of this research. Thirdly, partial volume artefact will have unavoidably been present, however the observers ensured they eroded the ROIs to avoid including bone as much as possible. The authors chose the trade-off between resolution to signal to noise ratio, which is always the consideration in MR imaging. Further developments will allow better spatial resolution in the future. Nevertheless, the methodology used to draw ROIs in the desired section of cartilage was robust and repeatable with an excellent intra-rater and inter-rater score [30].

The research has effectively validated a T2 mapping sequence on a 0.27 T MR system and showed that low field T2 mapping of the equine DIPJ was repeatable and reliable *ex vivo*. Furthermore, there

was a significant positive correlation between low and high field T2 measurements. Mean cartilage T2 relaxation time was shown to be significantly higher in the lateral section of the DIPJ compared to the medial section and there was a specific middle phalanx lateral lesion distribution identified which warrants further investigation.

Authors' declarations of interests

Steve Roberts is employed by Hallmarq Veterinary Imaging©. No other competing interests have been declared.

Ethical animal research

The study protocol was approved by the University of Edinburgh Veterinary Medicine Ethical Review Committee, ref: 9314 and 4.18.

Informed consent

Informed consent was obtained for all cases used in the study.

Data availability statement

The data that support the findings of this study are available from the corresponding author upon reasonable request

Source of Funding

M. Baker is funded through a Horse Trust PhD scholarship (G4018) and L. Kershaw is funded by GlaxoSmithKline. This work was supported by Hallmarq Veterinary Imaging. The National Research Foundation (NRF) of South Africa partly funded the histology costs.

Acknowledgements

We thank Hallmarq Veterinary Imaging© for support with MR scanning of the specimens in this study and for providing the T2 mapping sequence to use on the 0.27 T standing magnet; Linda George for her assistance with imaging the specimens; Chandra Logie, Craig Pennycook and Craig Johnstone from the University of Edinburgh for assisting with processing of the equine feet samples; Scott Maxwell, Sionagh Smith, Dawn Drummond and Gillian McGregor at Easter Bush Pathology for their

help and expertise with the histological sample processing and Dr Juliet Duncan and Dr Richard Reardon for statistical advice for this project.

Authorship

M. Baker, L. Kershaw and S. Taylor contributed to the study design, study execution, data analysis and interpretation, preparation of the manuscript and final approval of the manuscript. M. Baker had full access to all the data in the study and takes responsibility for the integrity of the data and the accuracy of the data analysis. A. Carstens, C. Daniel, H. Brown and S. Roberts contributed to the data analysis and interpretation, preparation of the manuscript and final approval of the manuscript.

Tables:

Table 1: Pulse sequence parameters for T2 mapping using the low field (0.27 T) and high field (3.0 T) MRI system.

Pulse sequence	Orientation	TE (ms)	TR (ms)	FOV (mm)	Matrix	Slice width (mm)	Voxel size (mm)	Space between slices (mm)	Scan time (min)
Low field: 2D multi-slice multi-echo spin echo	Dorsal	22, 44, 66, 88, 110	2000	210 x 210	256 x 256	3	0.82	0.9	08:00
High field: 2D multi-slice multi-echo spin echo	Dorsal	14, 28, 41, 55, 69	2440	140 x 140	384 x 384	3	0.36	0.0	08:15

Figure Legends:

Figure 1: The photograph demonstrates the 8 phantom tubes which each had different known T2 values placed inside a hoof coil in the 0.27 T open MR system for sequence validation.

Figure 2: Example of a dorsal low field MR scan of a left fore foot TE=22 ms image slice depicting the ROIs drawn where the histological samples were taken for comparisons between the medial (1) and lateral (2) condylar articular cartilage surfaces of the middle and distal phalangeal bones.

Figure 3: Measured T2 ± standard deviations vs. nominal T2 values. Close agreement is seen in the first 6 phantoms in the lower T2 range (50-150 ms). Orange line is the identity line.

Figure 4: The graph shows box plots of observer one's first T2 measurements for each OARSI grade (Obs A (1)), observer one's second T2 measurements (Obs A (2)) and observer two's T2 measurements (Obs B). Boxes show minimum T2, median with interquartile range and maximum T2.

Figure 5: The graphs show observer one's first lateral and medial T2 measurement (A), observer one's second lateral and medial T2 measurements (B) and observer two's lateral and medial T2 measurements (C).

Figure 6: (1) Photographs demonstrating the gross pathology of the articulating cartilage surface of the middle (P2) and distal (P3) phalangeal bones. The lateral condyle of P2 shows a large superficial abrasion (blue arrow) and there is also mild abrasion axially (black arrow). P3 shows normal smooth articular cartilage. The navicular bone is also shown in the image situated proximally to P3. (2) The dorsal T2 colour map of the left fore image slice from where the histological samples were taken depict increased T2 in the lateral condylar articular cartilage of P2 and articulating P3. (3) (A) H&E stained section taken from the lateral condylar surface of P2 demonstrates abnormal cartilage and disruption to the superficial cartilage layer (blue arrow). (B) Safranin O stained section shows advanced surface disruption of the superficial layer and loss of safranin O stain uptake in the superficial (1) middle (2) and deep (3) cartilage layers (black arrows) indicate proteoglycan loss, OARSI grade 3. (C) H&E stained section taken from the medial condylar surface of P2 shows minimal disruption to the superficial layer. (D) Safranin O stained section showing surface fibrillation and microscopic cracks in the superficial zone, OARSI grade 1.

Figure 7: The graphs show T2 measurements for OARSI grade 1 (A), grade 2 (B) and grade 3 (C) on the low field and high field system.

Figure 8: A case example of a right fore distal interphalangeal joint imaged on both the low (A) and high (B) field MR system. The transverse image is shown on the left, dorsal image in the centre and the corresponding dorsal T2 colour map on the right. The T2 colour map demonstrates increased T2 relaxation time in the lateral and medial articular cartilage of the middle and distal phalangeal bone condyles.

Figure 9: Bland-Altman plot showing the limits of agreement (dotted lines indicating the 95% confidence interval) between the low and high field T2 measurements.

References

1. Ireland JL, Clegg PD, McGowan CM, McKane SA, Chandler KJ, Pinchbeck GL. Disease prevalence in geriatric horses in the United Kingdom: veterinary clinical assessment of 200 cases. Equine Vet J, 2012;44(1):101-6.
2. McIlwraith CW. 3 - Traumatic Arthritis and Posttraumatic Osteoarthritis in the Horse. In: Joint Disease in the Horse (Second Edition), Eds: C.W. McIlwraith, et al. 2016, WB Saunders: Edinburgh. pp 33-48.
3. Brommer H, van Weeren PR, Brama PAJ, Barneveld A. Quantification and age-related distribution of articular cartilage degeneration in the equine fetlock joint. Equine Vet J, 2003;35(7):697-701.
4. Wilsher S, Allen WR, Wood JL. Factors associated with failure of thoroughbred horses to train and race. Equine Vet J, 2006;38(2):113-8.
5. van Zadelhoff C, Schwarz T, Smith S, Engerand A, Taylor S. Identification of Naturally Occurring Cartilage Damage in the Equine Distal Interphalangeal Joint Using Low-Field

Magnetic Resonance Imaging and Magnetic Resonance Arthrography. Frontiers in Veterinary Science, 2020;6:508.

6. Kaneene JB, Ross WA, Miller R. The Michigan equine monitoring system. II. Frequencies and impact of selected health problems. Prev Vet Med, 1997;29(4):277-92.
7. Keegan KG. Evidence-based lameness detection and quantification. Vet Clin North Am Equine Pract, 2007;23(2):403-23.
8. Colgate VA, T.F. Group, Marr CM. Science-in-brief: Risk assessment for reducing injuries of the fetlock bones in Thoroughbred racehorses. Equine Veterinary Journal, 2020;52(4):482-488.
9. Dyson PK, Jackson BF, Pfeiffer DU, Price JS. Days lost from training by two- and three-year-old Thoroughbred horses: a survey of seven UK training yards. Equine Vet J, 2008;40(7):650-7.
10. Hernandez J, Hawkins DL. Training failure among yearling horses. Am J Vet Res, 2001;62(9):1418-22.
11. Preston SA, Trumble TN, Zimmel DN, Chmielewski TL, Brown MP, Hernandez JA. Lameness, athletic performance, and financial returns in yearling Thoroughbreds bought for the purpose of resale for profit. J Am Vet Med Assoc, 2008;232(1):85-90.
12. Seitzinger AH, Traub-Dargatz JL, Kane AJ, Kopral CA, Morley PS, Garber LP, Losinger WC, Hill GW. A comparison of the economic costs of equine lameness, colic, and equine protozoal myeloencephalitis (EPM). Proceedings of the 9th International Symposium on Veterinary Epidemiology and Economics. 2000.
13. Murray RC, Mair TS, Sherlock CE, Blunden AS. Comparison of high-field and low-field magnetic resonance images of cadaver limbs of horses. Vet Rec, 2009;165(10):281-8.
14. Smith MA, Dyson SJ, Murray RC. Reliability of high- and low-field magnetic resonance imaging systems for detection of cartilage and bone lesions in the equine cadaver fetlock. Equine Vet J, 2012;44(6):684-91.

15. Evrard L, Audigié F, Bertoni L, Jacquet S, Denoix J-M, Busoni V. Low field magnetic resonance imaging of the equine distal interphalangeal joint: Comparison between weight-bearing and non-weight-bearing conditions. PLoS One, 2019;14(1):e0211101.

16. Mosher TJ, Dardzinski BJ. Cartilage MRI T2 relaxation time mapping: overview and applications. Semin Musculoskelet Radiol, 2004;8(4):355-68.

17. Schenk H, Simon D, Waldenmeier L, Evers C, Janka R, Welsch GH, Pachowsky ML. Regions at Risk in the Knee Joint of Young Professional Soccer Players: Longitudinal Evaluation of Early Cartilage Degeneration by Quantitative T2 Mapping in 3 T MRI. Cartilage, 2021;13(1_suppl):595s-603s.

18. Kretzschmar M, Nevitt MC, Schwaiger BJ, Joseph GB, McCulloch CE, Link TM. Spatial distribution and temporal progression of T2 relaxation time values in knee cartilage prior to the onset of cartilage lesions - data from the Osteoarthritis Initiative (OAI). Osteoarthritis Cartilage, 2019;27(5):737-745.

19. David-Vaudey E, Ghosh S, Ries M, Majumdar S. T2 relaxation time measurements in osteoarthritis. Magn Reson Imaging, 2004;22(5):673-82.

20. Liebl H, Joseph G, Nevitt MC, Singh N, Heilmeier U, Subburaj K, Jungmann PM, McCulloch CE, Lynch JA, Lane NE, Link TM. Early T2 changes predict onset of radiographic knee osteoarthritis: data from the osteoarthritis initiative. Ann Rheum Dis, 2015;74(7):1353-9.

21. Joseph GB, Baum T, Carballido-Gamo J, Nardo L, Virayavanich W, Alizai H, Lynch JA, McCulloch CE, Majumdar S, Link TM. Texture analysis of cartilage T2 maps: individuals with risk factors for OA have higher and more heterogeneous knee cartilage MR T2 compared to normal controls--data from the osteoarthritis initiative. Arthritis Res Ther, 2011;13(5):R153.

22. White LM, Sussman MS, Hurtig M, Probyn L, Tomlinson G, Kandel R. Cartilage T2 assessment: differentiation of normal hyaline cartilage and reparative tissue after arthroscopic cartilage repair in equine subjects. Radiology, 2006;241(2):407-14.

23. Menendez MI, Clark DJ, Carlton M, Flanigan DC, Jia G, Sammet S, Weisbrode SE, Knopp MV, Bertone AL. Direct delayed human adenoviral BMP-2 or BMP-6 gene therapy for bone and cartilage regeneration in a pony osteochondral model. Osteoarthritis Cartilage, 2011;19(8):1066-75.

24. Clark DJ, Jia G, Menendez MI, Choi S, Miller CJ, Sammet S, Flanigan DC, Bertone AL, Knopp MV. In Vivo Quantification of Cartilage Regeneration in an Equine Model at 3T Following Gene Therapy. In: Proceedings of the International Society for Magnetic Resonance in Medicine. 2010. p. 232.

25. Pownder S, Koff MF, Fortier L, Castiglione E, Saska R, Bradica G, Novakofski K, Potter HG. Quantitative and Morphologic Evaluation of Cartilage Repair in an Equine Model. In: Proceedings of the International Society for Magnetic Resonance in Medicine. 2011. p. 499.

26. Pritzker KPH, Gay S, Jimenez SA, Ostergaard K, Pelletier J-P, Revell PA, Salter D, van den Berg WB. Osteoarthritis cartilage histopathology: grading and staging. Osteoarthritis and Cartilage, 2006;14(1):13-29.

27. Schindelin J, Arganda-Carreras I, Frise E, Kaynig V, Longair M, Pietzsch T, Preibisch S, Rueden C, Saalfeld S, Schmid B, Tinevez J-Y, White DJ, Hartenstein V, Eliceiri K, Tomancak P, Cardona A. Fiji: an open-source platform for biological-image analysis. Nature Methods, 2012;9(7):676-682.

28. Rueden CT, Schindelin J, Hiner MC, DeZonia BE, Walter AE, Arena ET, Eliceiri KW. ImageJ2: ImageJ for the next generation of scientific image data. BMC Bioinformatics, 2017;18(1):529.

29. Schmidt K. MRIAnalysisPak Manual. 2004, Center for Comparative Neuroimaging (CCNI) at the University of Massachusetts Medical School and The Small Animal MRI Laboratory at Harvard Medical School/Brigham & Women's Hospital.

30. Koo TK, Li MY. A Guideline of Selecting and Reporting Intraclass Correlation Coefficients for Reliability Research. J Chiropr Med, 2016;15(2):155-63.

31. Johnston GCA, Ahern BJ, Woldeyohannes SM, Young AC. Does the Low-Field MRI Appearance of Intraosseous STIR Hyperintensity in Equine Cadaver Limbs Change when Subjected to a Freeze-Thaw Process? Animals (Basel), 2021;11(2):475.

32. Carstens A. Delayed gadolinium-enhanced magnetic resonance imaging and T2 mapping of cartilage of the distal metacarpus3/metatarsus3 of the normal Thoroughbred horse. 2013, University of Pretoria: South Africa.

33. Weaver RE, Sharif M, Livingston LA, Andrews KL, Fuller CJ. Microscopic change in macroscopically normal equine cartilage from osteoarthritic joints. Connect Tissue Res, 2006;47(2):92-101.

34. Chen M, Qiu L, Shen S, Wang F, Zhang J, Zhang C, Liu S. The influences of walking, running and stair activity on knee articular cartilage: Quantitative MRI using T1 rho and T2 mapping. PLoS One, 2017; 12(11):e0187008.

35. Mosher TJ, Smith HE, Collins C, Liu Y, Hancy J, Dardzinski BJ, Smith MB. Change in Knee Cartilage T2 at MR Imaging after Running: A Feasibility Study. Radiology, 2005;234(1):245-249.

36. Brommer H, van Weeren PR, Brama PA. New approach for quantitative assessment of articular cartilage degeneration in horses with osteoarthritis. Am J Vet Res, 2003;64(1):83-7.

37. Madsen SJ, Patterson MS, Wilson BC. The use of India ink as an optical absorber in tissue-simulating phantoms. Phys Med Biol, 1992;37(4):985-93.

38. Chang DG, Iverson P, Schinagl RM, Sonoda M, Amiel D, Coutts RD, Sah RL. Quantitation and localization of cartilage degeneration following the induction of osteoarthritis in the rabbit knee. Osteoarthritis Cartilage, 1997;5(5):357-72.

39. Clayton HM. Biomechanics of the Distal Interphalangeal Joint. Journal of Equine Veterinary Science, 2010;30(8):401-405.

40. Dippel M, Ruczizka U, Valentin S, Licka TF. Influence of Increased Intraarticular Pressure on the Angular Displacement of the Isolated Equine Distal Interphalangeal Joint. Journal of Equine Veterinary Science, 2016;38:54-63.

41. Paggi E, Laus F, Cerquetella M, Spaterna A, Tesei B. Intra-Articular Pressure in the Horse. Israel Journal of Veterinary Medicine, 2012;67(3):142-23.

42. Viitanen MJ, Wilson AM, McGuigan HR, Rogers KD, May SA. Effect of foot balance on the intra-articular pressure in the distal interphalangeal joint in vitro. Equine Vet J, 2003;35(2): 184-9.

43. Denoix J. Functional anatomy of the equine interphalangeal joints. In: Proc. Am. Assoc. Equine Practnrs. 1999. Citeseer.

44. Chateau H, Degueurce C, Jerbi H, Crevier-Denoix N, Pourcelot P, Audigié F, Pasqui-Boutard V, Denoix J-M. Three-dimensional kinematics of the equine interphalangeal joints: articular impact of asymmetric bearing. Veterinary Research, 2002;33(4):371-382.

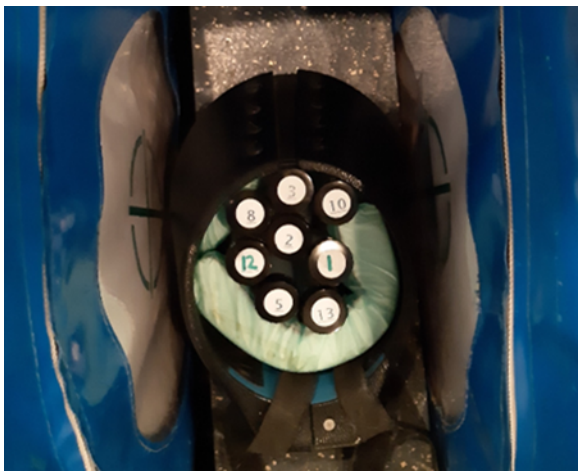

EVJ_13900_Figure 1 Photograph phantom tubes.tif

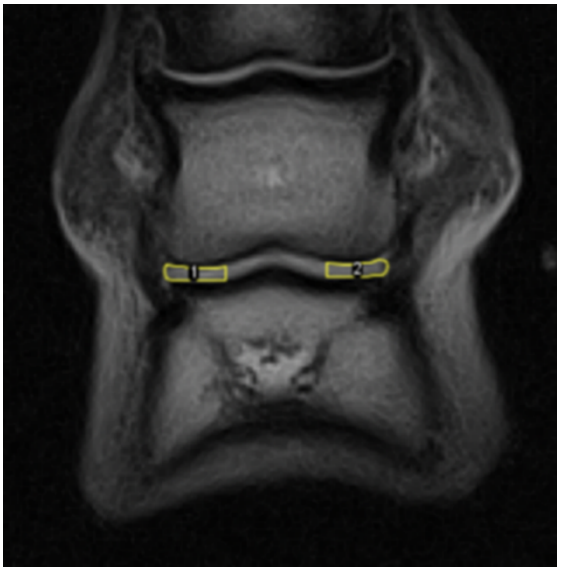

EVJ_13900_Figure 2 ROI position.tif

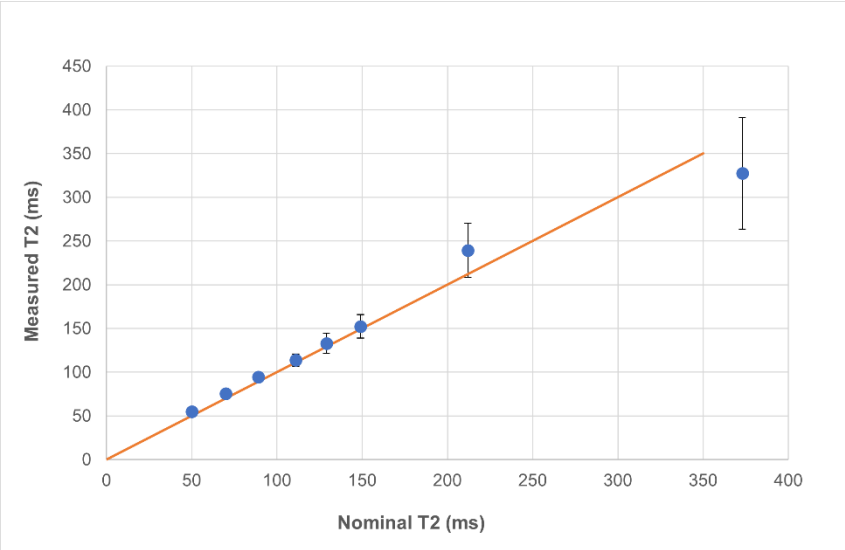

EVJ_13900_Figure 3 nominal and measured T2.tif

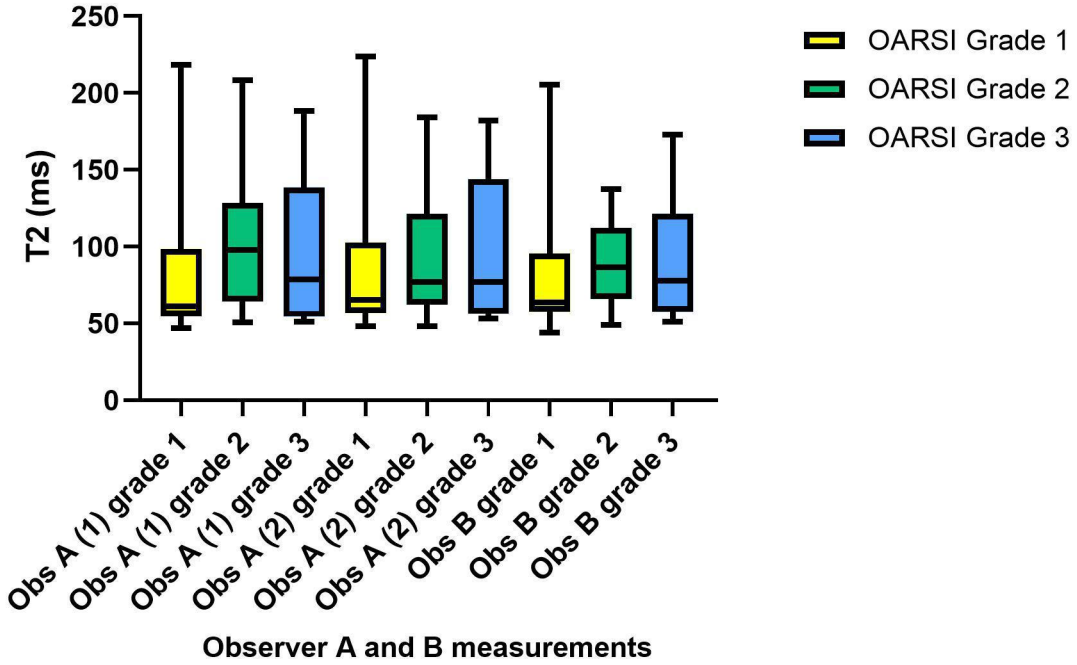

EVJ_13900_Figure 4.jpg

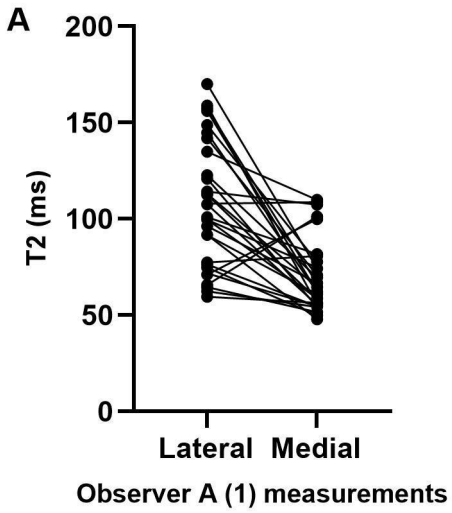

EVJ_13900_Figure 5A.jpg

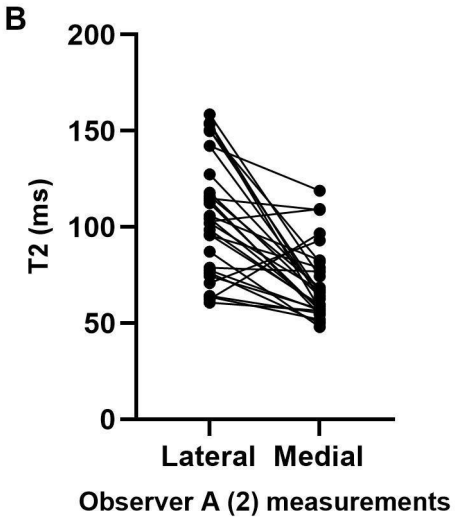

EVJ_13900_Figure 5B.jpg

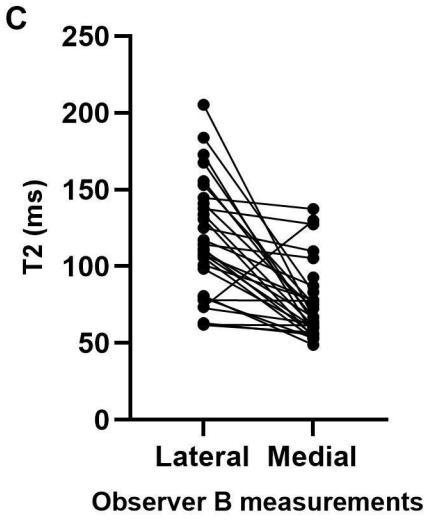

EVJ_13900_Figure 5C.jpg

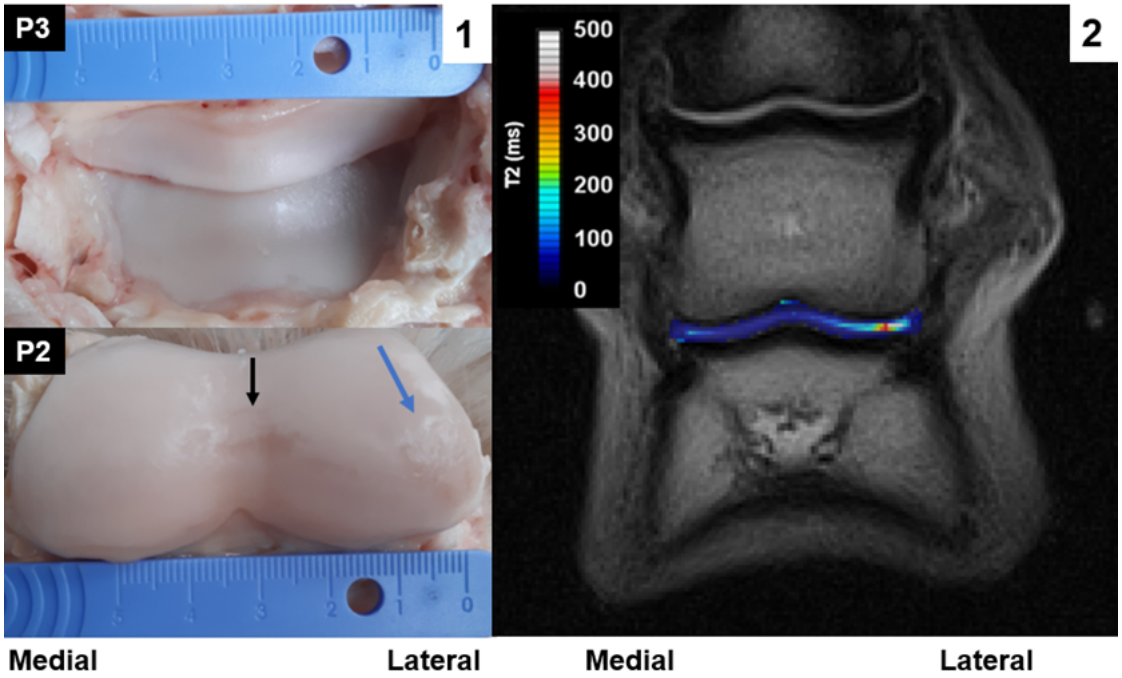

EVJ_13900_Figure 6_1 and 2.tif

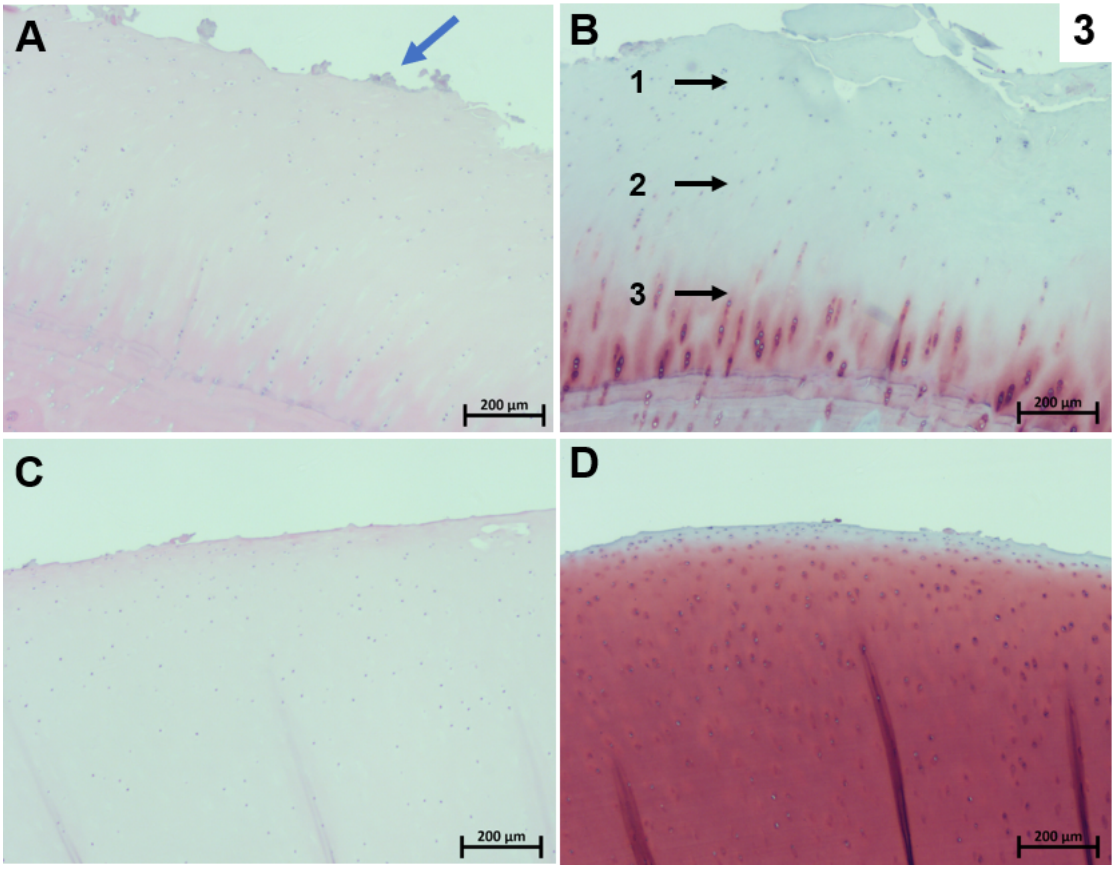

EVJ_13900_Figure 6 _3.tif

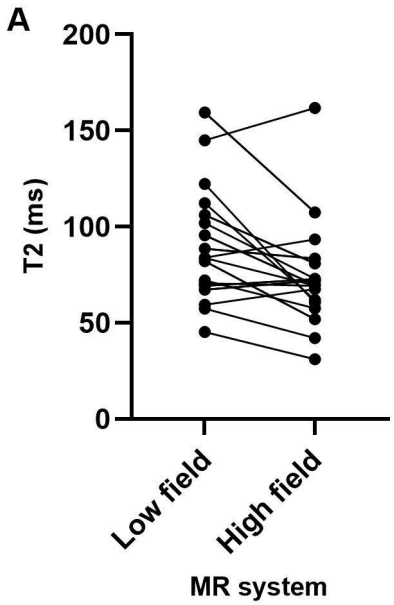

EVJ_13900_Figure 7A.jpg

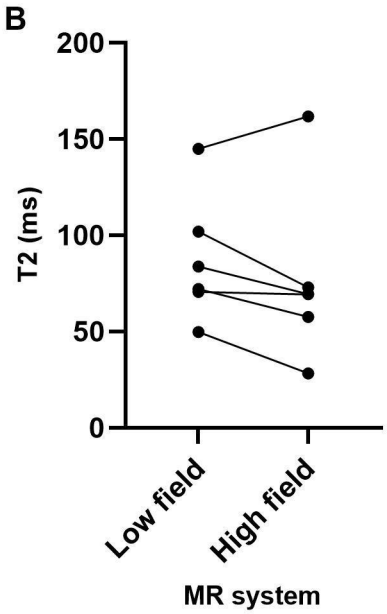

EVJ_13900_Figure 7B.jpg

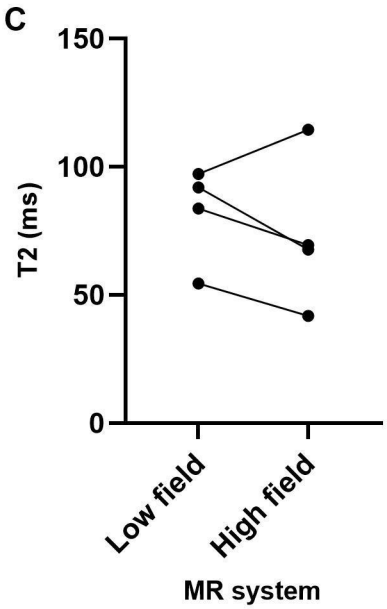

EVJ_13900_Figure 7C.jpg

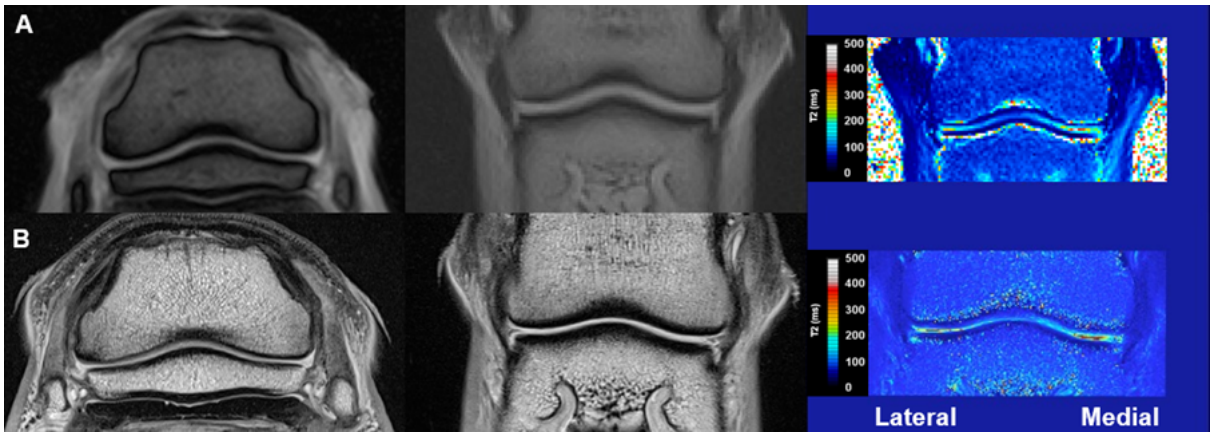

EVJ_13900_Figure 8.tif

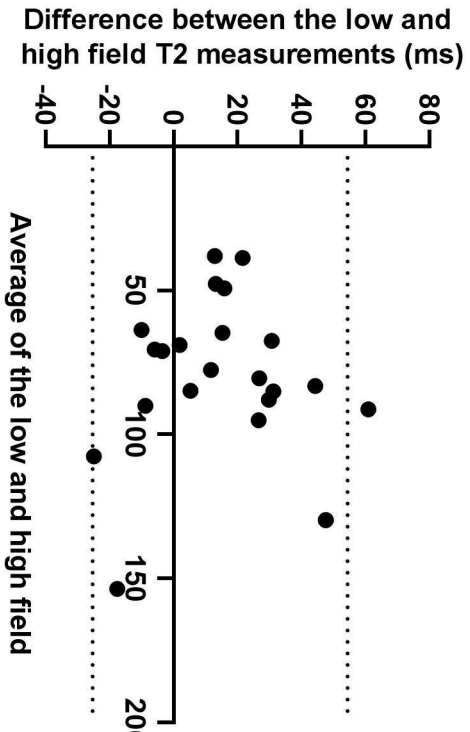

EVJ_13900_Figure 9.jpg